Testing and Validation Methodology for a Radiation Monitoring System for Electronics in Particle Accelerators

Alessandro Zimmaro, Rudy Ferraro, Jérôme Boch, Frédéric Saigné, Rubén García Alía, *Member, IEEE*, Matteo Brucoli, Alessandro Masi, and Salvatore Danzeca

***Abstract*— In this work, a methodology for the design and validation of a radiation monitoring (RadMON) system for electronic systems in particle accelerators is presented. The methodology expands the common radiation hardness assurance (RHA) procedure implemented at CERN, including new steps dedicated to both system-level testing, focused on a wireless device, and sensors characterization and readout validation. A case study demonstrating the validity of this methodology is proposed with the qualification of a novel battery-powered wireless RadMON system. This system not only represents the validation vehicle of the methodology but also an innovation in terms of monitoring platform due to its flexibility and improved capabilities. The application of this methodology allowed its full qualification, providing useful data in terms of resistance to radiation, lifetime, and failure rate in operation, demonstrating the validity of the testing strategy proposed in the article.**

***Index Terms*— High energy hadrons, radiation hardness assurance (RHA), radiation monitoring (RadMON), system level testing, thermal neutrons (ThNs), total ionizing dose (TID).**

I. Introduction

AT CERN, the Large Hadron Collider (LHC) hosts many electronic systems based on components off the shelf (COTS) that are exposed to a mixed radiation field. The energy spectra of particles at LHC can range from a few megaelectronvolt thermal neutrons (ThNs) to the gigaelectronvolt range [1], [2] and as a result, these components can be affected by all radiation effects at the same time: displacement damage (DD), total ionizing dose (TID), and single event effects (SEEs) [3], [4]. Systems and components that are exposed to these harsh environments must be adequately tested and qualified so that their expected lifetime and failure rate are known. To avoid unexpected failures during operation, qualification steps and associated testing are required. Space Agencies provide their own radiation hardness assurance (RHA) procedures and guidelines in order to standardize these strategies such as [5] and [6]. Several articles, available in the literature, expand these procedures by discussing, for example, the risk management and assessment approaches, as in [7], or through the authors' experience, by highlighting challenges and providing advice, as in [8], where the author's goal is to provide tips on how to perform radiation qualification for components and systems. In addition, innovative testing modalities are available in the literature, which can improve the qualification process, such as the "Tri-flux" test developed by the Jet Propulsion Laboratory (JPL) [9]–[11]. It allows understanding if an implemented mitigation scheme in the system is flux-dependent [12]. Another alternative approach to system-level radiation testing is proposed in [13] and demonstrated to simulate the effect of component level TID degradation on system performance.

At CERN, systems are qualified by following the RHA procedure [14], [15] which provides steps to follow and recommendations to ensure reliable qualification for CERN radiation environments. For instance, it was shown in [16] that for optoelectronic devices the standard test with protons did not give reliable results due to nonionizing energy loss (NIEL) scaling violations with neutrons, which constitute the majority of the particles in the LHC environment. Furthermore, it was shown in [17] that bipolar or BiCMOS integrated circuits (ICs) could exhibit completely different degradation profiles depending on when exposed to different ratios of TID and DD rates as is in the case of the LHC and thus representative ratios should be used during testing. Finally, it was also pointed out in [18] the presence of ThNs in the areas of the LHC could significantly contribute to the overall SEE and devices should be also qualified against them to allow a reliable estimation of the failure rate in operation.

All these dedicated test methodologies included in the CERN RHA have further improved the reliability of the qualification process nowadays. However, the procedure can be further improved by adding another layer of qualification to the generic RHA procedure for some specific application-related challenges. Such a dedicated set of procedures targeting only these specific challenges will ensure another level of reliability that is needed currently due to the increase of radiation levels

Manuscript received 8 October 2021; revised 29 January 2022 and 1 March 2022; accepted 4 March 2022. Date of publication 10 March 2022; date of current version 18 July 2022. This work was supported by the French National Program "Programme d'Investissement d'Avenir. IRT Nanoelec" under Grant ANR-10-AIRT-05.

Alessandro Zimmaro is with the European Organization for Nuclear Research (CERN), 1211 Geneva, Switzerland, and also with IES–UMR UM/CNRS 5214, Université de Montpellier, 34095 Montpellier, France (e-mail: alessandrozimmaro@gmail.com).

Rudy Ferraro, Rubén García Alía, Matteo Brucoli, Alessandro Masi, and Salvatore Danzeca are with the European Organization for Nuclear Research (CERN), 1211 Geneva, Switzerland.

Jérôme Boch and Frédéric Saigné are with IES–UMR UM/CNRS 5214, Université de Montpellier, 34095 Montpellier, France.

Color versions of one or more figures in this article are available at https://doi.org/10.1109/TNS.2022.3158527.

Digital Object Identifier 10.1109/TNS.2022.3158527

that will come with the high luminosity LHC (HL-LHC) update [14].

Therefore, this article proposes to extend this generic RHA with an additional level of qualification with dedicated test methodologies for radiation monitoring (RadMON) systems. RadMON activities are crucial tasks at CERN and while the complexity of the systems follows increasing requirements, their reliability in operation must be maintained or even increased. Today at CERN, increasing requirements in terms of flexibility, coverability, radiation tolerance, and radiation sensor capabilities have motivated the development of a battery-powered, radiation-tolerant wireless RadMON platform. This new wireless monitoring system architecture implies several design choices and working modes that need to be assessed during the qualification process with dedicated test methodologies to ensure system reliability. Specific system-level requirements such as the need to work in a strong duty cycle mode, imply specific working conditions at the component level that need to be assessed early in the RHA process.

Accordingly, in this article, a methodology for the design and validation of a RadMON system for electronic systems in particle accelerators is presented. The methodology expands the common RHA procedure implemented at CERN by including application-specific steps dedicated to the challenges above mentioned, focusing on a wireless device, and sensor characterization and readout validation. The recently developed battery-powered wireless radiation monitoring system (BatMon) is used as a case study to demonstrate the validity of the proposed methodology. This system is not only the vehicle for validating the methodology but also an innovation in terms of monitoring platform due to its flexibility and enhanced capabilities.

II. Platform Design Choices and Challenges

The general requirements for the design of a battery-powered wireless monitoring system, combined with the specific radiation tolerance requirements for a system exposed to intense radiation, lead to several design choices that, in turn, impose some new radiation qualification challenges to be evaluated. These design choices that have driven the development of the CERN Battery-powered radiation Monitoring (BatMon) system and the associated qualification challenges are described in Sections II-A–II-F. In this article, the dose is given in Gy(Si), although the unit reported is Gy for conciseness.

A. System Modularity

The first requirement for the system is modularity. The objective, in addition to designing a flexible and easily maintainable radiation system, is also to provide to the CERN users a generic monitoring platform that can be used for a wide variety of projects. Therefore, the system is built on four printed circuits: 1) the powerboard; 2) the main-board; 3) the sensor board; and 4) the deported module. While the first two boards are application-independent, the two last depend on the application, in the case of this work, the RadMON. The PowerBoard hosts up to four 7.2 V Lithium batteries that provide a capacity of 17 A $\times$ h. The Main-Board hosts several

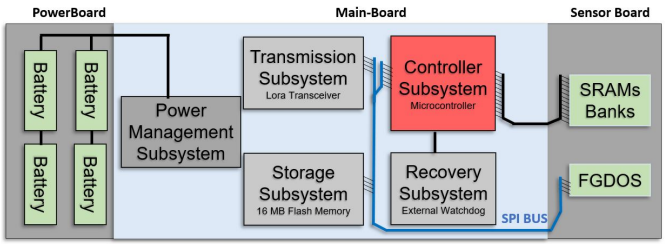

Fig. 1. Conceptual diagram of the BatMon System.

subsystems: the Controller Subsystem, the Transmission Subsystem (a wireless transceiver), the Storage Subsystem, the Recovery Subsystem, and the Power Management Subsystem.

The latter consists of two linear regulators connected to the PowerBoard and providing low noise 5 and 3.3 V dc voltages, which are also needed for the Sensor Board. In addition, a MOSFET and bipolar junction transistor (BJT) design allows reading the three different power rails (low-dropout regulators (LDOs)' output and Battery Voltage) through resistor dividers without losing in power consumption. A conceptual diagram of the Main-Board is shown in Fig. 1.

B. Low Power Components

The expected long lifetime of the system (several years) imposes strong low power requirements and therefore components have to be chosen according to low power specification: low leakage current, low quiescent currents. However, this is not enough and, to lower the average consumption, even more, the use of a duty cycle mode (wake, measure, store and transmit information, sleep) must be implemented. This specific type of working mode imposes in return extra requirements on the choice of components, such as the presence of low power modes or the need for the radiation sensors to cumulate and store data by working principle.

C. Communication Technology

Flexibility, low power requirements, and wide-area coverage (LHC) are typical constraints of the Internet of Things (IoT). In addition to these, radiation tolerance complicates the search for a suitable wireless technology. The Long Range (LoRa) technology, which is widely used in IoT applications, seems to be the best choice and meets the requirements [19].

However, being a commercial solution, radiation effects can lead the transceiver to not be able to connect or transmit, which can imply the need for dedicated mitigation measures. On the other hand, being a wireless solution, the possibility of network unavailability or a low received signal strength indication (RSSI) could lead to packets loss and thus, measurements. Therefore to improve the reliability of the system, it was decided to embed a Storage Subsystem made of 16 MB serial peripheral interface (SPI) nonvolatile Flash memory to store information in case of wireless communication unavailability due to radiation effects or network unavailability. In addition, LoRa features such as Confirmed Uplink and Adaptive Data Rate can be used to improve the reliability of the system.

D. Controller Choice

The choice of the Controller Subsystem, which is interfaced together with the sensors and the communication module,

is consequently constrained by the lower power requirements and its compatibility with the LoRa module. The field-programmable gate array (FPGA) is the natural choice of controller for radiation designs. It offers a large number of general purpose input–outputs (GPIOs), high flexibility in the hardware, which allows the development of complex design and mitigation techniques such as triple modular redundancy (TMR). On the other hand, microcontrollers (MCUs) give less flexibility in hardware design and rely on sequential operations. However, they provide already embedded peripherals such as analog to digital converter (ADC), Real-Time Clock, and SPI Bus useful for controlling sensors and onboard hardware. In addition, they offer power-saving modes that allow attainment of low power requirements not achievable with an FPGA. The lack of mitigation techniques requires the use of an external watchdog to improve the reliability of the system and restore its functionality in case of a single event functional interrupt (SEFI). This results in the need to find an additional component that meets all the requirements already mentioned. However, the existence of libraries to control the LoRa transceiver along with the low power capabilities pushed the choice of the MCU.

E. Radiation Sensor

The choice of the radiation sensors is driven by the same requirements of low power, duty cycle mode compatibility, and interface compatibility with the MCUs. At the same time, they should provide the measurement of metrics of interest for the CERN accelerators, such as TID, DD, high energy hadrons (HeH), and ThNs as shown in [14]. For this purpose, the sensors currently used in the CERN RadMON represented a good starting point. In the RadMON [20], two different well-calibrated parallel static random access memories (SRAMs), whose sensitivity to both ThN and HeH is known, allow retrieving the different fluences by combining their measurements as shown in [20]. Since the search for candidate SPI SRAMs providing the same capabilities is still ongoing, we chose to keep the same memories in the BatMon. However, the limited number of input–outputs (IOs) in the MCU imposed the use of SPI IO expanders to cope with the parallel interface of the SRAMs.

Concerning the TID, the RadFets used on the RadMON require a complex circuitry made of several components that are relatively power consuming and not easily replaceable. On the other hand, CERN has been collaborating for many years on the development of a new fully digital Floating Gate DOSimeters (FGDOS) [21] that does not require any external circuitry. Its SPI bus and different working modes such as passive mode fit perfectly with the system requirements. The device offers a higher TID resolution than the RadFet, allowing measurements in places where the latter would not be able to measure, such as in the shielded areas of the LHC where the dose rate is less than 10 Gy per year [14].

III. Dedicated RHA Concerns

The design choices presented above imply several qualification challenges that are inherent to this family of wireless and low power systems, and that are not considered in the traditional CERN RHA. These challenges, therefore, imply dedicated test and validation methodologies that complement the generic CERN RHA procedure, making it suitable for full validation of a RadMON system. The proposed additional testing methodologies take place in three phases of the traditional RHA. First, in the component level qualification phase, dedicated test methodologies and concerns are added to those already defined for CERN radiation environments. Second, in the electrical validation phase, new functional tests are added from which the primary information for system radiation qualification is extracted. Third, at the system level qualification phase, tests under different types of particle spectra are proposed to obtain the performance degradation, expected lifetime, and failure rate information that will define the use of the system and possible improvements for it. Finally, the sensor calibration phase, which is not considered by the CERN RHA since sensors are a specific feature of the system, is added as a final qualification step to complete the methodology. All these phases and their challenges are discussed in Sections III-A–III-E.

A. Component Qualification

At CERN, as is the case for this monitoring system, systems can be highly distributed, and thus, the use of qualified COTS [22] components is the preferred solution. The CERN RHA standard already provides valuable information on component test methodologies, and the CERN database provides a wide selection of qualified components for a broad range of applications. However, very few low power and wireless applications were developed at CERN in the previous years, and thus, few suitable components were available in the database for such applications. In addition, test methodologies may not be adapted to them. Low power components can embed several internal features such as power saving, different operational or sleeps modes, and also work with much lower internal biasing. Therefore, such components might exhibit higher degradation and more failure modes, which, together with the high radiation levels expected for the HL-LHC, up to 100 Gy and 10^{11} 1 MeV $n_{eq} \cdot cm^{-2}$ per year in the tunnel [14], made the search for a suitable candidate challenging.

Therefore, several recommendations should be followed when testing such components. Considering that other effects such as dose rate effects are handled in the test, the usual worst case biasing during tests might lead to overestimated component degradation rates compared to the one expected in operation. For this reason, it is more reasonable to have test conditions similar to those in operation, keeping in mind that it may lower the radiation margin and thus imply greater confidence in the obtained responses. In the case of battery-powered applications, the devices will be in sleep or off most of the time, which can have a great impact on the lifetime. Examples of the impact of the biasing conditions are shown in Section III-B.

B. System Electrical Validation

Not all system features require radiation testing to be validated, such as duty cycle life, transmission capacity, and storage functionality. Evaluation of these electrical parameters

can have a great impact on subsequent system-level testing under radiation. For example, lifetime as a function of duty cycle also defines the subsequent use of the device, as it allows us to know those "real working conditions" that will allow us to perform a more realistic test of the system under radiation.

C. Functional and System Validation

Reproducing at the component level the dynamic biasing that systems will face during their lifetime is something complex and difficult to foresee. This is even more true for low power components where the biasing conditions are drastically dependent on the working modality of the system, such as the value of the duty cycle. Besides, systems will face both TID and DD whose ratio can lead to unexpected components degradation of and failure [4]. Finally, not all the functionalities can be tested at the component level. For example, mitigation techniques such as the external watchdog to restore the MCU functionalities or the communication link reliability when both the MCU and the LoRa module are exposed can only be tested at the system level. Proper system validation can prove the correct functionality of the sensors and test their degradation with radiation and with the degradation of the system itself. In addition, system-level testing allows knowing the real radiation tolerance and sensitivity of the system. The above-mentioned reasons demonstrate the need for system-level validation, which allows qualifying functionalities and parameters that are not possible to verify at the component level. However, during system-level qualification, it is necessary to consider some aspects that may lead to nullifying the quality and the validity of the tests.

A complex system is made of different subsystems, which may exploit different working modalities during operation. In particular, the system might exploit the worst case operating condition for different subsystems not during the same work phase. To overcome this problem, test the system using a duty cycle mode could represent a solution. However, this is not enough unless followed by the choice of a realistic duty cycle. Thus, if possible, the system should be tested by emulating, as much as possible, the behavior it will have during real operation [23]. Choosing to test the system using a duty cycle mode without properly selecting the correct facility can lead to test invalidation. The flux is an important parameter in this choice [24]. Testing using a pulsed beam is risky because it is possible that, using a realistic duty cycle, not all operating conditions will be tested correctly if there is no synchronization between system and beam. Another important feature of the flux is its tunability. Systems based on digital circuits such as MCUs and FPGA could be strongly influenced by the beam flux. Keeping in mind that the system should be tested using realistic duty cycle conditions if the flux is too high, it might not be able to exploit all the different working conditions, restarting or stopping to work before the end of a complete working cycle. Also, in this case, not all the operating conditions would be tested and thus, the system would not be fully qualified. On the other hand, since the beam time in most of the facilities is limited, it is not possible to test using low flux and achieving high fluence and dose at the same time. A possible solution, which is explained in Section V-F, is to test the system in a hybrid way: ramping up the flux through different runs to estimate the SEE cross section with a low flux and then, check the lifetime using the highest one. In this way, it is possible to test the system sensitivity exploiting all the working conditions and reach a high Dose Level in an acceptable time. Finally, high observability of the electrical parameter during all tests, as stressed in [25], will allow us to know the cause of the failure and improve the system in the future.

D. Choice of the Appropriate Facility

Several possibilities exist to perform validation at the system or subsystem level under radiation. The best candidate for complete system validation at CERN is the CERN High energy AcceleRator Mixed field (CHARM) facility [26], which provides the opportunity to test complete electronic systems within a realistic field that is fully representative of the mixed field environment of the high energy accelerator. However, provided CHARM is not always available, this qualification phase can be split into different validation steps through the use of other facilities.

Co-60 facilities are perfect for a first qualification phase: they allow to test only TID monitoring performances of the entire system combining the different system and sensor working modes to verify the accuracy achieved. In addition, the only gamma contribution in the spectrum allows exploiting all the working modalities of the system without having to worry about the reset or SEFI problem that occurs in the case of CHARM. Moreover, testing in a Co-60 source enables the possibility of easily fine-tuning the dose rate allowing investigating dose-rate effects.

The high-energy proton beams such as the one used by CERN for component level tests are also a good solution to test small systems or perform subsystem testing against SEE, TID, and DD combined. At Paul Scherrer Institute (PSI) [27], even if the beam is continuous and slightly tunable, the limited beam time and the high proton flux can make it necessary to adopt the precautions described above. Besides, by using an appropriate flux, it is also possible to validate the HeH fluence sensor readout capability.

Finally, as defined in [14] and [18], the HL-LHC will host, such as the LHC, areas where the contribution of ThN is greater than the one of HeH. Single-event upset (SEU) susceptibility generated by ThN has been reported since the 1980s for several electronic components containing Boron 10 (B10), in boron-polysilicon glass (BPSG) layers, boron-doped p-type silicon [28], [29]. In general, there is no information about the fabrication process for COTS and thus, a system based on this type of component could be sensitive to ThN effects. This sensitivity could lead the system to soft errors (recoverable - partial loss of the functionality). To avoid unexpected behavior, a system test under ThN is necessary to know its sensitivity under this type of particles spectrum. In addition, the ThN fluence measurement capability can be validated.

Finally, bipolar component degradation profiles can be strongly affected by the TID/DD ratio. Thus, it is important to test in ratios representative to the ones present in the LHC

environments [4]. Proton irradiations allow to cover a part of the ratios present in the LHC but the most representative ones can be obtained with neutron irradiation from nuclear reactors or the mixed-fields of the CHARM facility. This also applies at the system level since the system itself can exhibit different performances degradation profiles if it embeds both MOSFET and bipolar-based components.

E. Sensor Calibration

While according to the accelerator RHA, high-energy proton testing (up to at least 200 MeV) is usually sufficient to evaluate both SEE and TID sensitivity of the components, in the case of radiation sensors, finer characterization is required. For the SRAM, for example, the objective is to measure SEU cross sections both for ThN and HeH. For the former, the calibration is performed at the Institut Laue-Langevin (ILL) in Grenoble [30], France. While for HeH, the cross section is characterized at the PSI in Villigen, Switzerland, under a high-energy proton beam of 200 MeV [27]. Then, in the case of FGDOS, which incorporates several working modes, it is important to evaluate the impact of the different modes in terms of resolution, accuracy, and sensitivity degradation. For this specific sensor, this analysis was performed in our previous work [19] and extended during this work through the study of the passive mode. And the degradation of the sensor in terms of current consumption and sensitivity in this operating mode.

For the sensor calibrations, two different approaches can be followed. Typically, a lot qualification is performed in which the average sensitivity and dispersion of radiation responses are measured against the different radiation effects. However, it is sometimes possible to calibrate each system to increase the accuracy of the measurements by acquiring the real sensitivity of each system's sensors. Such a methodology is usually too complex to implement since testing many systems requires a lot of cabling, but, in the case of wireless battery-powered applications, the only difficulty is in calibrating the test positions. An example of such a process is shown in Section V-G.

IV. System Validation

The additional validation and qualification steps added to the standard RHA were applied to the BatMon system to validate it. This system represents the validation vehicle for the methodology and innovation in terms of monitoring platform. In this section, several testing approaches are proposed that complete the methodology by allowing reproducibility of operations for a different system and proving its validity.

A. Component Level Qualification

As presented in Section III-A, the first step in the proposed methodology is the qualification at the component level. We considered it as a requirement to have a replacement rate of failed units of one every three years, which corresponds for the most difficult areas, the dispersion suppressor (DS), to a dose of about 300 Gy [14]. Among the tested components, some have presented interesting qualification requirements and results. For instance, the 16 MB NOR Flash Memory used in the BatMon to store the data in case of communication unavailabilities or losses, has shown different failure levels depending on its operation mode. This component offers three different modalities of work: Active, OFF, Deep Power Mode. During the test, nine memories, divided into groups of 3 (One working modality per group), were initialized with a fixed pattern and were checked at different dose steps. Table I shows the highest doses at which communication with the Flash memory was still possible. As visible in Table I, in OFF mode the Flash Memories survived up to doses 2.5 times higher than in deep power mode, which has the mode expected to be used. These results demonstrate that for the low power components the biasing conditions are fundamental. For the system keeping the memory ON is not an option in terms of consumption, while having the memory OFF is the only way to comply with the target TID and therefore it requires to have the possibility of the system to power OFF only this device. Nonetheless, the lifetime in operation has to be tested accordingly to the duty cycle, which can be performed at the system level. Other interesting results were the fact that both the MCU and LoRa transceiver were exhibiting failures and the functionalities can be restored only through a power cycle. The LoRa transceiver was shown to have a SEFI cross section of $3.51 \cdot 10^{-11}$ cm^2, which motivates the use of an external watchdog to Recover the system in the case of SEFI.

TABLE I
Flash Memories TID Failure Level

Modality	Active	OFF	Deep Power
Dose [Gy]	400	>500	200

B. Power Requirements Validation

As described in Section III-B, some tests can be performed without radiation to evaluate if the performance of the system meets the original requirements, such as expected system life based on power consumption. The BatMon implements the duty cycle mode described in Section II-B which allows reducing the daily energy consumed and improves the Battery Lifetime. In Fig. 2, the current consumption of the system is depicted. As it is possible to see, during sleep the power saving mode of the controller and the different components allow reaching current values much lower than the one requested during the measuring period. The reading cycle depends on how coarse or fine the measurements are required. Increasing the number of measurements, thus, reducing the duty cycle, the system battery lifetime is reduced. This counter effect is visible in Fig. 3, where the expected system lifetime, calculated through the data relating to the current consumption of the system, is represented as a function of the duty cycle. With these design choices, the system will be capable of working for more than three years in LHC areas where the daily dose is lower than 20 Gy/year and a high duty cycle can be used. As will be shown in the next paragraph, low dose rates (LDRs) effects lead to an increase in the current consumption of the system that results in a reduction in terms of its battery life as the dose rate increases, testifying, the necessity of the evaluation of the same performances under radiation as defined in Section III-B.

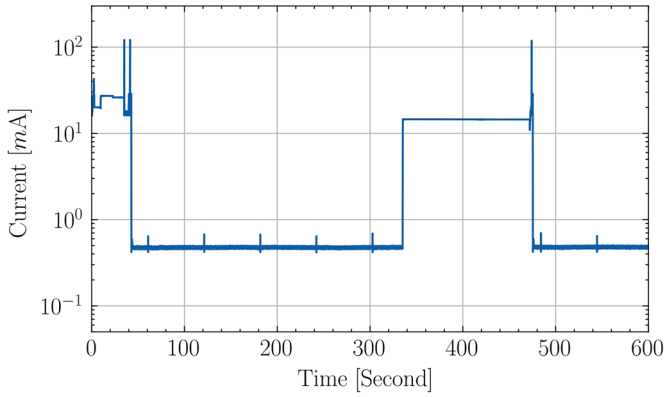

Fig. 2. BatMon current consumption. After an initial boot period, the device sleeps for a configurable period. At its end, it wakes up, measures, sends, and back to sleep. Afterward, the cycle repeats.

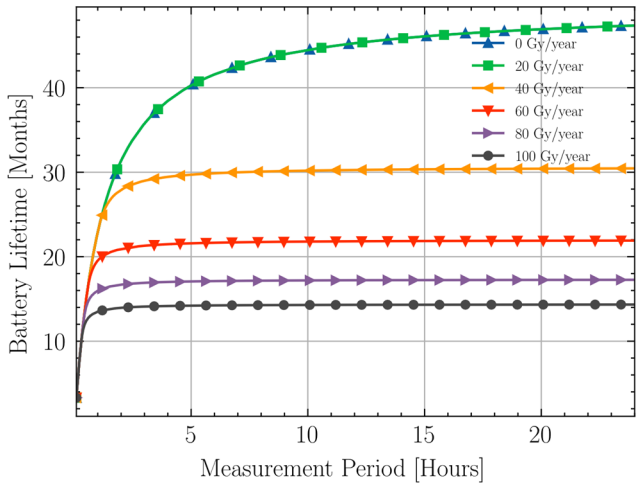

Fig. 3. Battery lifetime is directly proportional to the measurement period chosen. The expected dose rate per year can influence the lifetime leading to an independence from the measurement period.

C. System-Level Validation Under TID

As described in Section III-D, the unavailability of CHARM makes necessary more tests in different types of facilities to complete the qualification of the system. As foreseen from the methodology, the evaluation of the system's degradation performance under the only TID has been carried out at the Co-60 facility which represents a perfect test environment to evaluate it, since the Gamma contribution cannot generate any SEFI in the system allowing to test all the operations without interruptions. Different tests were performed to validate and qualify the system.

As defined in Section III-C, the choice of a realistic duty cycle between the different operating modes can lead the system to different performance degradation. Since the BatMon is supposed to work most of the time in sleep compared to the active phase (Measuring every 1 h or once per day), an initial test was performed to verify the system TID degradation and sensor sensitivity with two different duty cycles. The duty cycle (DC_{Bat}) of the BatMon can be defined as follows:

$$DC_{Bat} = \frac{T_{Sleep}}{T_{Active}}$$

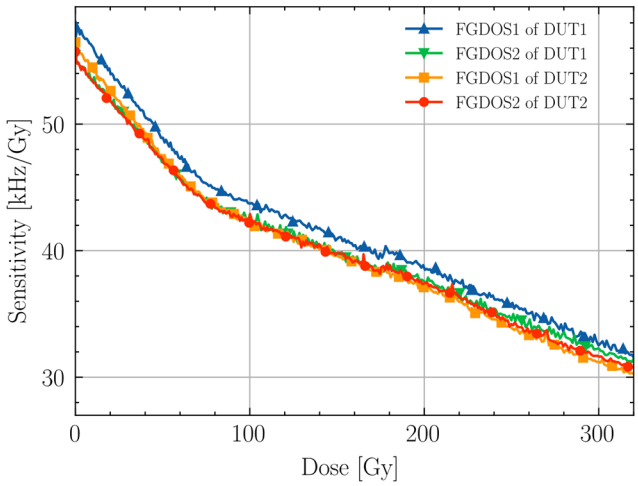

Fig. 4. In passive mode the FGDOS sensitivity degrades with the TID. It is not depending on DC_{Bat} chosen.

where T_{Sleep} is the amount of time spent in sleep and T_{Active} is the amount of time in active mode. During the active phase, the BatMon spends most of the time reading the memories. For this reason, one BatMon was programed with the basic firmware (DUT1), having a DC_{Bat} of ∼50%. The second one (DUT2) was programed instead with a modified firmware in which the Controller Subsystem was only reading the FGDOS during the active phase reducing drastically the duration of the active phase and leading the DC_{Bat} to ∼85%. The devices were placed in front of the beam and the dose rate was set to 3.06 Gy/h. An indoor LoRaWAN Gateway RAK7258 was configured to provide the LoRa network while the packets received were logged in specific log files. The test lasted a few days, once reached the dose of 320 Gy they were removed. At the end of the test, the devices were still functional. The Flash memory that in the BatMon exploits both the Active and Deep power state was still working. The sensitivity degradation of the FGDOS was investigated to check the impact of the DC_{Bat} used. The behavior is depicted in Fig. 4 and as it is visible, the slope of the curve is reduced at around 80 Gy. In addition, the base current required by the two systems was increased by a similar offset at the end of the test. The increase was due to the sensor board and was not depending on the operation conditions (Sleep or active). To check which component was consuming more, the 5 V line, which was powering the FGDOS, was cut and the individual component was powered from another supply. The FGDOS was the source of the current increase.

To investigate the increase of the current consumption another test was carried out. This time two devices (DUT3 and DUT4) were irradiated and the current consumption was recorded every second. As explained in Section III-D, the possibility to test the full duty cycle of the system without interruptions in the system functionality is a feature of this facility and it is perfect to perform a qualification of the performance degradation due to only TID. The devices were placed in front of the beam and the dose rate was set to 3.96 Gy/h. The test lasted a few days. Once they reached the dose of 350 Gy, they were removed. The current increased

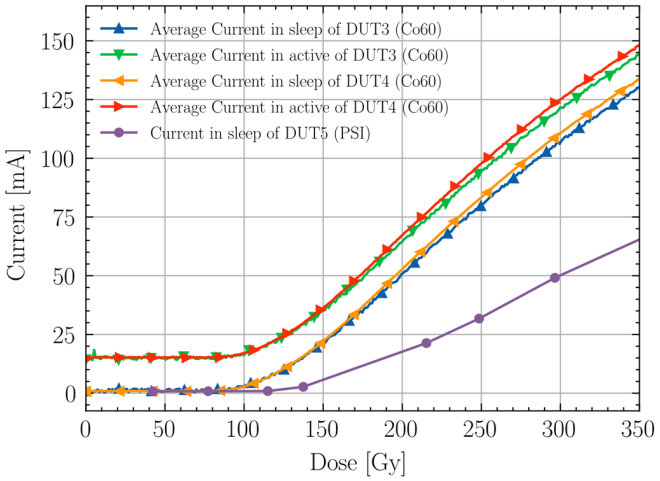

Fig. 5. Current consumption of the system is increasing as the TID increase. After ∼80 Gy starts slowly increasing and reaching a slope of 0.5 mA/Gy at ∼150 Gy. The current increase is compared with the one observed under high dose rate (>46 Gy/h) at PSI (DUT5).

behavior was analyzed and is shown in Fig. 5. Through this data, it was possible to compute the real-life operation. As visible in Fig. 3, where the dose rate is less than or equal to 20 Gy/year, the lifetime of the BatMon is not affected by the current consumption increase. In the harshest environment like the DS area of LHC where the expected dose rate is around 100 Gy/year, the BatMon is still capable of working more than one year but above a measurement period of 1 h, the lifetime is independent of this parameter. These results provided a comprehensive view of system performance degradation, testifying to the importance of this step in the methodology and its validity.

D. System-Level Validation Under ThN

Once the TID performance degradation was known, the BatMon has been qualified under a Thermal and Epi-Thermal Neutron beam at the ILL institute in Grenoble, France. The institute hosts a new beamline called Thermal and Epi-Thermal Neutron irradiation Station (TENIS), which has been readapted for Radiation to electronics qualification. It can provide to the test area a neutron field with a fission spectrum extracted from the reactor core. Gold foil activation calibrations conducted by the institute attested that the equivalent flux of ThN (normalized to 25 meV) is $2.8 \cdot 10^9$ n/cm^2/s. This flux consists of 60% ThNs and 40% epithermal neutrons. Since the entire system does not fit in the irradiated area and the total SEE sensitivity is the sum of all the sensitivity of each subsystem, the different subsystems were tested one by one but always with the full system in operation. This test method allowed identifying in which subsystems the problem occurs and to complete component level tests if not performed. The fluence reached, shown in Table II, was chosen according to the higher probability of having B10 effects in Transmission and Controller Subsystems. For the Controller and Transmission subsystem, the fluence accumulated is higher than that expected in one year of operation in the DS area ($2 \cdot 10^{11}$ n/cm^2) [14], ensuring no failure in operation for this type of particle spectrum in this harsh area.

TABLE II
DIFFERENT SUBSYSTEMS WERE TESTED THROUGH SHORT RUNS WITHSTANDING DIFFERENT FLUENCES WITHOUT SHOWING ANY SENSITIVITY TO ThN

SubSystem under test	Fluence absorbed [n/cm^2]
Transmission Subsystem	$1.35 \cdot 10^{12}$
Controller subsystem	$1.14 \cdot 10^{12}$
Recovery Subsystem	$4.61 \cdot 10^{11}$
Power Management Subsystem	$4.06 \cdot 10^{10}$

TABLE III
RECOVERABLE CROSS SECTION EVALUATED AT DIFFERENT FLUX FOR TWO DIFFERENT BATMON

Flux [p/(s·cm^2)]	BatMon1 Recoverable Faults Cross-section [cm^2]	BatMon2 Recoverable Faults Cross-section [cm^2]
$2.2 \cdot 10^7$	$6.5 \cdot 10^{-11}$	$3.25 \cdot 10^{-11}$
$6.89 \cdot 10^7$	$5.81 \cdot 10^{-11}$	$2.33 \cdot 10^{-11}$
$1.51 \cdot 10^8$	$3.49 \cdot 10^{-11}$	$3.49 \cdot 10^{-11}$
$2.31 \cdot 10^8$	$1.73 \cdot 10^{-11}$	$1.52 \cdot 10^{-11}$

E. System-Level Validation Under HeH, TID, and DD

The proposed methodology foresees a final test campaign under HeH necessary to complete the system sensitivity assessment and estimate the failure rate in operation. The test was carried out at PSI which is used also for component evaluation. The beam offered by this facility has two important features highlighted in Section III-D: a continuous and tunable flux. However, although the latter features can help in testing a system based on MCU and FPGA exploiting the full duty cycle, the beam time is limited and thus, a different testing approach has to be applied to evaluate both the cross section and the degradation under TID and DD of the system. Since it was not possible to irradiate all the subsystems together, it was decided to test more subsystems together keeping always under irradiation the MCU. From the data obtained from component level qualification, it was known that the two components sensitive to HeH were the Transmission and the Controller subsystems. Thus, one BatMon was irradiated by having in beam the Controller with the Transmission and the Power Management Subsystems (BatMon1) while the other having Controller with the Recovery and the Storage Subsystems (BatMon2). As anticipated in Section III-C, a hybrid solution was exploited ramping up the flux after a certain TID. During the test, the MCU was allowed to check all the subsystem functionalities helping to solve observability problems. In addition, the reset line and the power rails were checked using an oscilloscope. The different runs are reported in Table III with the corresponding cross section evaluated for each system. As visible, the BatMon1 cross section decreases with the increase of the flux. This behavior is justified by the use of an external Watchdog as a mitigation technique. The recovery time from the appearance of a SEFI can vary from a few seconds to a minute because an external Watchdog monitors the state of the MCU with a fixed given time interval. In addition, the use of software mitigation techniques implemented within the MCU means that it can also reset itself, reducing this time to a few milliseconds. For these

reasons, when using a high flux, some SEFIs can be masked by the long recovery time combined with the high flux and thus, not be visible and quantifiable. It can be observed that the cross section of BatMon1 is always higher concerning the one of BatMon2. Since no single event transient (SET) causing reset was observed on the Regulators, the cause of this higher failure rate can be attributed to the Transmission Subsystem, which can stop work as the Controller Subsystem for SEFIs. At 275 Gy, the BatMon2 stops working because of permanent failure in the External Watchdog, which kept the reset line low. This component is a perfect example concerning what was said in Section III-D since its lifetime turns out to be strongly influenced by the DD dose (DDD)/TID ratio. When tested at Co60 Facility, where the DDD/TID ratio is two orders of magnitude lower [17], they were failing at about 500 Gy.

At the end of the test, the BatMon1 showed a failure that was only recovered through a power cycle. The not-recoverable faults cross section is $9.32 \cdot 10^{-13}$ cm^2/device. The current increase was observed and evaluated also in this High Dose-Rate context and is shown in Fig. 5. The increase was lower and it was not possible to acquire complete cycles because of the SEFIs occurring. LDR seems to be the criticality for the Current Increase. As said in Section III-D, Co60 allows better evaluation of TID Performance degradation respect to Mixed-effects facilities such as PSI. Since the External Watchdog was able to recover the system but was working below the desired target Dose, another test was carried out enabling the internal watchdog, irradiating the most sensitive portion of the system (Same of BatMon1). The same approach described in the previous test was performed. However, the internal watchdog solution was discarded since it was not always able to recover the system showing a Not-Recoverable Faults Cross section of $1.18 \cdot 10^{-11}$ cm^2/device. These results obtained using this testing approach allow evaluation of the failure rate in operation testifying to the importance of this phase within the methodology and its validity. Using the collected data, it is possible to estimate the probability of the system failure rate for specific HL-LHC environments and years of operation using the homogeneous Poisson process (HPP). This process considers a constant failure rate and independence between each failure.

The DS and Arc areas, which are two unshielded areas of the accelerator where the electronic equipment is installed, were considered for this analysis, and the predicted failure rate for one year of operation is depicted in Fig. 6. In the shielded areas, where the BatMon will be mostly used, the radiation levels in terms of HeH fluence per year, are expected to be less than or of the same order as the Arc area, which represents the worst case scenario for these areas. As visible in Fig. 6, the probability of having a permanent failure is negligible within the Arc area.

This type of failure analysis can also be done for a space environment by considering the radiation parameters obtained through a specific software such as Outil de Modélisation de l'Environnement Radiatif Externe (OMERE) as done in [31].

F. System Calibration

Section III-E discussed the improvement in terms of accuracy measurements lead performing calibration specifically

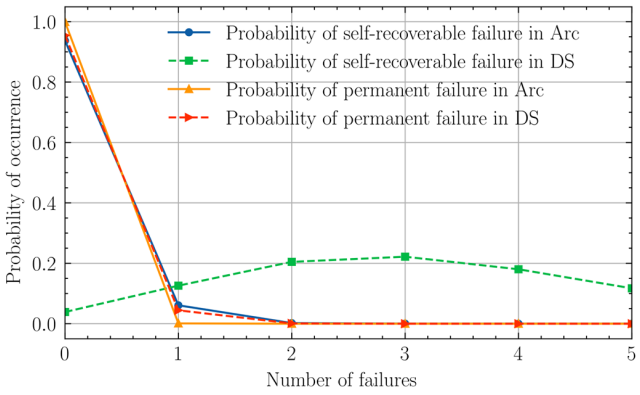

Fig. 6. Probability of having a self-recoverable failure in Arc (HeH = 10^9 p/cm^2) in one year of operation is 5%, while for a permanent failure it is negligible (<0.1%). In the harshest environment like DS (HeH = $5 \cdot 10^{10}$ p/cm^2), this probability increases reaching for permanent failure 5% while for self-recoverable failure 20% of having 2 or 3 resets per year [14].

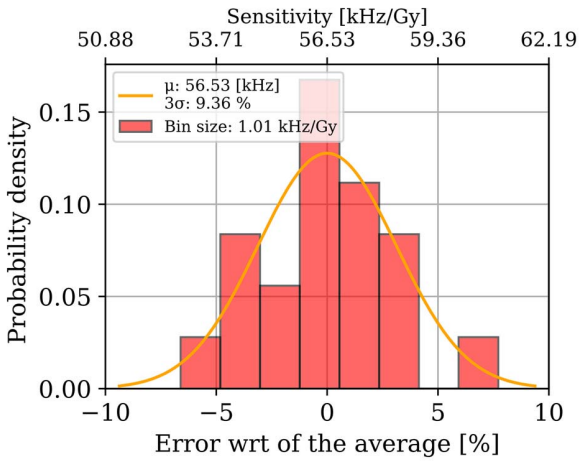

Fig. 7. Probability density of the measured FGDOS TID sensitivity and error made with respect of an experimental average value.

for each device. In particular, it emphasizes the difficulty to define a methodology since common systems require cabling or complex setup while in contrast a methodology can be defined for a wireless battery-powered monitoring system. The first calibration was carried out at the Co-60 facility on the TID sensor, the FGDOS. Ten BatMons were irradiated and the dose rates at each FGDOS position were measured by a 1cc Ionization Chamber (PTW 23331). The resulting FGDOS sensitivity distribution is shown in Fig. 7. For three-sigma, the dispersion is about 10%, which therefore defines the uncertainty of the system measurement if average sensitivity is used. However, thanks to the flexibility of the system this procedure was rather simple to be performed and can therefore be part of a methodic calibration procedure that can drastically improve the measurement accuracy in operation.

V. Conclusion

In this article, a new methodology for testing and validation of a RadMON system has been presented. The methodology extends the RHA procedure implementing new steps and validation phase which are specific for this type of system. To prove its validity, the different phases proposed in Section III have been applied on the BatMon which represents

an innovation in terms of monitoring platform for its flexibility and improved capabilities. Different test approaches have been described during the article through which it has been possible to evaluate the different performances degradation and the failure rate of the system. The use of this methodology made it possible to evaluate different degradation aspects of the system such as the reduction of the lifetime as the cumulative dose increases, the independence of the degradation from the chosen duty cycle, and the bottleneck of the system (the Recovery Subsystem at 275 Gy). At the same time test approach in ThN and HeH beams allowed us to know the sensitivity of the system and its recoverable and not-recoverable faults cross section, Thanks to this data it has been possible to evaluate the failure rate in operation, as shown in Section IV-E. The data presented in this article will be representative of the deployed parts in an initial deployment phase, where no more than 30 samples will be involved. Therefore, the number of samples tested is sufficient to ensure the reliability of the system. In the future, larger-scale production and deployment are expected, so testing will continue at CHARM and involve more samples.

Nowadays, BatMons are fully qualified and are used for real measurements in super proton synchrotron (SPS). In the future, they will be installed in the LHC where the LoRa Network is available. Improved version of the system in terms of sensors and Main-Board, that will solve the weakness highlighted thanks to the test approach provided by the proposed methodology, are in development.

ACKNOWLEDGMENT

The authors would like to thank the Institut Laue-Langevin (ILL), for the beamtime allocated INDU-225.

REFERENCES

[1] K. Roeed, M. Brugger, and G. Spiezia, "An overview of the radiation environment at the LHC in light of R2E irradiation test activities," CERN, Geneva, Switzerland Tech. Rep. CERN-ATS-Note-2011-077, 2011. [Online]. Available: https://cds.cern.ch/record/1382083

[2] K. Bilko *et al.*, "Radiation environment in the LHC arc sections during run 2 and future HL-LHC operations," *IEEE Trans. Nucl. Sci.*, vol. 67, no. 7, pp. 1682–1690, Jul. 2020, doi: 10.1109/TNS.2020.2970168.

[3] R. G. Alía *et al.*, "Single event effects in high-energy accelerators," *Semicond. Sci. Technol.*, vol. 32, no. 3, Feb. 2017, Art. no. 034003. [Online]. Available: https://iopscience.iop.org/article/10.1088/1361-6641/aa5695/meta

[4] R. Ferraro *et al.*, "Study of the impact of the LHC radiation environments on the synergistic displacement damage and ionizing dose effect on electronic components," *IEEE Trans. Nucl. Sci.*, vol. 66, no. 7, pp. 1548–1556, Jul. 2019, doi: 10.1109/TNS.2019.2902441.

[5] ESA/ESCC Basic Specification, *Single Event Effects Test Methods and Guidelines*, ESA, Noordwijk, The Netherlands, document 25100, 2005.

[6] C. Poivey, "Radiation hardness assurance for space systems," NASA, USA, Tech. Rep., 2002. [Online]. Available: https://ntrs.nasa.gov/api/citations/20020080842/downloads/20020080842.pd

[7] K. A. LaBel, A. H. Johnston, J. L. Barth, R. A. Reed, and C. E. Barnes, "Emerging radiation hardness assurance (RHA) issues: A NASA approach for space flight programs," *IEEE Trans. Nucl. Sci.*, vol. 45, no. 6, pp. 2727–2736, Dec. 1998, doi: 10.1109/23.736521.

[8] H. Quinn, "Challenges in testing complex systems," *IEEE Trans. Nucl. Sci.*, vol. 61, no. 2, pp. 766–786, Apr. 2014, doi: 10.1109/TNS.2014.2302432.

[9] J. A. Zoutendyk, H. R. Schwartz, R. K. Watson, Z. Hasnain, and L. R. Nevill, "Single-event upset (SEU) in a dram with on-chip error correction," *IEEE Trans. Nucl. Sci.*, vol. NS-34, no. 6, pp. 1310–1315, Dec. 1987, doi: 10.1109/TNS.1987.4337471.

[10] G. R. Allen, L. Edmonds, C. W. Tseng, G. Swift, and C. Carmichael, "Single-event upset (SEU) results of embedded error detect and correct enabled block random access memory (Block RAM) within the Xilinx XQR5 VFX130," *IEEE Trans. Nucl. Sci.*, vol. 57, no. 6, pp. 3426–3431, Dec. 2010, doi: 10.1109/TNS.2010.2085447.

[11] G. Allen *et al.*, "Single event test methodologies and system error rate analysis for triple modular redundant field programmable gate arrays," *IEEE Trans. Nucl. Sci.*, vol. 58, no. 3, pp. 1040–1046, Jun. 2011, doi: 10.1109/TNS.2011.2105282.

[12] S. M. Guertin, "SOC SEE test guideline development," presented at the Single-Event Effects Symp., La Jolla, CA, USA, 2013.

[13] A. F. Witulski *et al.*, "Simulation of transistor-level radiation effects on system-level performance parameters," *IEEE Trans. Nucl. Sci.*, vol. 66, no. 7, pp. 1634–1641, Jul. 2019, doi: 10.1109/TNS.2019.2922903.

[14] R. G. Alía *et al.*, "LHC and HL-LHC: Present and future radiation environment in the high-luminosity collision points and RHA implications," *IEEE Trans. Nucl. Sci.*, vol. 65, no. 1, pp. 448–456, Jan. 2018, doi: 10.1109/TNS.2017.2776107.

[15] S. Uznanski *et al.*, "Qualification of electronic components for a radiation environment: When standards do not exist—High-energy physics," CERN, Geneva, Switzerland, Tech. Rep., 2017. [Online]. Available: https://cds.cern.ch/record/2765495

[16] R. Ferraro *et al.*, "COTS optocoupler radiation qualification process for LHC applications based on mixed-field irradiations," *IEEE Trans. Nucl. Sci.*, vol. 67, no. 7, pp. 1395–1403, Jul. 2020, doi: 10.1109/TNS.2020.2972777.

[17] R. Ferraro, R. G. Alía, S. Danzeca, and A. Masi, "Analysis of bipolar integrated circuit degradation mechanisms against combined TID–DD effects," *IEEE Trans. Nucl. Sci.*, vol. 68, no. 8, pp. 1585–1593, Aug. 2021, doi: 10.1109/TNS.2021.3082646.

[18] M. Cecchetto *et al.*, "Thermal neutron-induced SEUs in the LHC accelerator environment," *IEEE Trans. Nucl. Sci.*, vol. 67, no. 7, pp. 1412–1420, Jul. 2020, doi: 10.1109/TNS.2020.2997992.

[19] K. Mekkia, E. Bajica, F. Chaxela, and F. Meyerb, "A comparative study of LPWAN technologies for large-scale IoT deployment," *ICT Exp.*, vol. 5, no. 1, pp. 1–7, Mar. 2019, doi: 10.1016/j.icte.2017.12.005.

[20] G. Spiezia *et al.*, "A new Radmon version for the LHC and its injection lines," *IEEE Trans. Nucl. Sci.*, vol. 61, no. 6, pp. 3424–3431, Dec. 2014, doi: 10.1109/TNS.2014.2365046.

[21] M. Brucoli *et al.*, "Investigation on passive and autonomous mode operation of floating gate dosimeters," *IEEE Trans. Nucl. Sci.*, vol. 66, no. 7, pp. 1620–1627, Jul. 2019, doi: 10.1109/TNS.2019.2895366.

[22] F. Faccio, "COTS for the LHC radiation environment: The rules of the game," in *Proc. 6th Workshop Electron. LHC Exp.*, Oct. 2000, pp. 50–65.

[23] M. Rousselet, P. C. Adell, D. J. Sheldon, J. Boch, H. Schone, and F. Saigne, "Use and benefits of COTS board level testing for radiation hardness assurance," in *Proc. 16th Eur. Conf. Radiat. Effects Compon. Syst. (RADECS)*, Sep. 2016, pp. 118–122, doi: 10.1109/RADECS.2016.8093122.

[24] A. Coronetti *et al.*, "Radiation hardness assurance through system-level testing: Risk acceptance, facility requirements, test methodology, and data exploitation," *IEEE Trans. Nucl. Sci.*, vol. 68, no. 5, pp. 958–969, May 2021, doi: 10.1109/TNS.2021.3061197.

[25] T. Rajkowski *et al.*, "Comparison of the total ionizing dose sensitivity of a system in package point of load converter using both component- and system-level test approaches," *Electronics*, vol. 10, no. 11, p. 1235, May 2021, doi: 10.3390/electronics10111235.

[26] J. Mekki, M. Brugger, R. G. Alia, A. Thornton, N. C. Dos Santos Mota, and S. Danzeca, "CHARM: A mixed field facility at CERN for radiation tests in ground, atmospheric, space and accelerator representative environments," *IEEE Trans. Nucl. Sci.*, vol. 63, no. 4, pp. 2106–2114, Aug. 2016, doi: 10.1109/TNS.2016.2528289.

[27] W. Hajdas, F. Burri, C. Eggel, R. Harboe-Sorensen, and R. de Marino, "Radiation effects testing facilities in PSI during implementation of the Proscan project," in *Proc. IEEE Radiat. Effects Data Workshop*, Jul. 2002, pp. 160–164, doi: 10.1109/REDW.2002.1045547.

[28] J. L. Autran, S. Serre, S. Semikh, D. Munteanu, G. Gasiot, and P. Roche, "Soft-error rate induced by thermal and low energy neutrons in 40 nm SRAMs," *IEEE Trans. Nucl. Sci.*, vol. 59, no. 6, pp. 2658–2665, Dec. 2012, doi: 10.1109/TNS.2012.2222438.

[29] A. Hands *et al.*, "Single event effects in power MOSFETs due to atmospheric and thermal neutrons," *IEEE Trans. Nucl. Sci.*, vol. 58, no. 6, pp. 2687–2694, Dec. 2011, doi: 10.1109/TNS.2011.2168540.

[30] J. Beaucour *et al.*, "Grenoble large scale facilities for advanced characterisation of microelectronics devices," in *Proc. 15th Eur. Conf. Radiat. Effects Compon. Syst. (RADECS)*, Sep. 2015, pp. 312–315, doi: 10.1109/RADECS.2015.7365616.

[31] R. Secondo *et al.*, "System level radiation characterization of a 1U CubeSat based on CERN radiation monitoring technology," *IEEE Trans. Nucl. Sci.*, vol. 65, no. 8, pp. 1694–1699, Aug. 2018, doi: 10.1109/TNS.2018.2797319.